



# Pharmacokinetics and pharmacogenetics of high-dose methotrexate in Chinese adult patients with non-Hodgkin lymphoma: a population analysis

Lin Yang<sup>1</sup> · Hui Wu<sup>2</sup> · Brenda C. M. de Winter<sup>3</sup> · Chang-cheng Sheng<sup>4,5</sup> · Hong-qiang Qiu<sup>6</sup> · Yu Cheng<sup>6</sup> · Juan Chen<sup>1</sup> · Qiu-ling Zhao<sup>1</sup> · Jing Huang<sup>1</sup> · Zheng Jiao<sup>4,7</sup> · Rui-xiang Xie<sup>1</sup>

Received: 29 December 2019 / Accepted: 12 March 2020 / Published online: 3 April 2020  
© Springer-Verlag GmbH Germany, part of Springer Nature 2020

## Abstract

**Purpose** High-dose methotrexate (HD-MTX) is widely used in the treatment of non-Hodgkin lymphoma (NHL), but the pharmacokinetic properties of HD-MTX in Chinese adult patients with NHL have not yet been established through an approach that integrates genetic covariates. The purposes of this study were to identify both physiological and pharmacogenomic covariates that can explain the inter- and intraindividual pharmacokinetic variability of MTX in Chinese adult patients with NHL and to explore a new sampling strategy for predicting delayed MTX elimination.

**Methods** A total of 852 MTX concentrations from 91 adult patients with NHL were analyzed using the nonlinear mixed-effects modeling method. *FPGS*, *GGH*, *SLCO1B1*, *ABCB1* and *MTHFR* were genotyped using the Sequenom MassARRAY technology platform and were screened as covariates. The ability of different sampling strategies to predict the MTX concentration at 72 h was assessed through maximum a posteriori Bayesian forecasting using a validation dataset (18 patients).

**Results** A two-compartment model adequately described the data, and the estimated mean MTX clearance (CL) was 6.03 L/h (9%). Creatinine clearance (CrCL) was identified as a covariate for CL, whereas the intercompartmental clearance (Q) was significantly affected by the body surface area (BSA). However, none of the genotypes exerted a significant effect on the pharmacokinetic properties of MTX. The percentage of patients with concentrations below 0.2  $\mu\text{mol/L}$  at 72 h decreased from 65.6 to 42.6% when the CrCL decreased from 90 to 60 ml/min/1.73 m<sup>2</sup> with a scheduled dosing of 3 g/m<sup>2</sup>, and the same trend was observed with dose regimens of 1 g/m<sup>2</sup> and 2 g/m<sup>2</sup>. Bayesian forecasting using the MTX concentrations at 24 and 42 h provided the best predictive performance for estimating the MTX concentration at 72 h after dosing.

**Conclusions** The MTX population pharmacokinetic model developed in this study might provide useful information for establishing personalized therapy involving MTX for the treatment of adult patients with NHL.

**Keywords** Methotrexate · Non-Hodgkin lymphoma · NONMEM · Pharmacogenomics · Population pharmacokinetics

✉ Zheng Jiao  
zjiao@fudan.edu.cn

✉ Rui-xiang Xie  
rxr\_fch@163.com

<sup>1</sup> Department of Pharmacy, Fujian Cancer Hospital & Fujian Medical University Cancer Hospital, Fuma Road 420, Fuzhou 350014, China

<sup>2</sup> Department of Medical Oncology, Fujian Cancer Hospital & Fujian Medical University Cancer Hospital, Fuzhou, China

<sup>3</sup> Department of Hospital Pharmacy, Erasmus MC, University Medical Center Rotterdam, Rotterdam, The Netherlands

<sup>4</sup> Department of Pharmacy, Huashan Hospital, Fudan University, 12 Middle Urumqi Road, Shanghai 200040, China

<sup>5</sup> Department of Pharmacy, Guizhou Provincial People's Hospital, Guiyang, China

<sup>6</sup> Department of Pharmacy, Fujian Medical University Union Hospital, Fuzhou, China

<sup>7</sup> Department of Pharmacy, Shanghai Chest Hospital, Shanghai Jiao Tong University, No. 241 West Huaihai Road, Shanghai 200030, China

## Introduction

High-dose methotrexate (HD-MTX), a folic acid antagonist, serves as the cornerstone in the treatment of non-Hodgkin lymphoma (NHL) because it prevents and treats neuromeningeal localization [1].

MTX is approximately 60% protein-bound [2], competing with the enzymes of the folate cycle, including methylene tetrahydrofolate reductase (MTHFR) [3], for active transport across cell membranes through a single carrier-mediated active transport process. MTX undergoes intracellular metabolism by folylpolyglutamate synthetase (FPGS) to obtain polyglutamated MTX, and this form can be converted back to MTX by hydrolase enzymes (GGH). Small amounts of MTX polyglutamates might remain in the tissue for extended periods [4]. MTX can be pumped out of the cell by ATP-binding cassette (ABC) and transported to hepatocytes for elimination by organic anion transporting polypeptide (OATP) 1B1, which is encoded by the *ABCB1* and *SLCO1B1* genes, respectively [5, 6]. After intravenous infusion, 80–90% of the MTX dose is excreted unchanged in the urine within 24 h, whereas 10% or less of the dose is eliminated through biliary excretion [7].

However, treatment is often limited by severe systemic toxicity [1], which is related to exposure to MTX [8]. Delayed MTX elimination is defined as a serum MTX concentration above 50  $\mu\text{mol/L}$  at 24 h, above 5  $\mu\text{mol/L}$  at 48 h, or above 0.2  $\mu\text{mol/L}$  at 72 h [4]. Patients that experience delayed MTX elimination are at elevated risk of toxicity, such as gastrointestinal toxicity, myelosuppression, mucositis, neurotoxicity, and liver and kidney dysfunction, which explains the importance of routinely monitoring the MTX concentration to guide leucovorin rescue and avoid potential side effects until the plasma concentrations decrease to below the threshold value of 0.2  $\mu\text{mol/L}$ .

The clearance of MTX exhibits a large interindividual variability, which leads to different exposures to the drug and can thus affect the clinical outcomes of the patients [9, 10]. Therefore, the determination of individual pharmacokinetic (PK) parameters, such as through maximum posterior Bayesian (MAPB) estimation, are needed for the optimization of individual therapy.

Pharmacogenomics studies have demonstrated that the disposition, efficacy, and toxicity of MTX can be influenced by single-nucleotide polymorphisms (SNPs) in the following genes: *FPGS* and *GGH* (which encode metabolizing enzymes of MTX), *SLCO1B1* and *ABCB1* (which encode transporters of MTX), and *MTHFR* (which encodes a target of MTX) [11–13]. Taking *SLCO1B1* as an example, a previous study showed that the plasma concentration

of MTX at 48 and 72 h is increased significantly in individuals with *SLCO1B1* rs4149056 variant (TC/CC genotype) compared with the wild-type individuals (TT genotype). Patients with the rs4149056 C allele exhibit a significantly higher frequency of adverse effects [14]. The significant association of *SLCO1B1* rs4149056 with the serum MTX levels was also observed by Csordas et al. [15], and Lima et al. [16] and Avivi et al. [17] who also demonstrated that *SLCO1B1* rs4149056 is associated with MTX-related toxicity. Lopez et al. [18] found a statistically significant association between the plasma concentration of MTX and *SLCO1B1* rs11045879, and Li et al. obtained the same result [19]. Further investigations on whether these SNPs in related genes explain the interindividual variability in MTX pharmacokinetics are required prior to the inclusion of genetic information in MTX individual therapy.

The majority of population pharmacokinetic (PPK) studies on MTX have focused on acute lymphocytic leukemia (ALL) in children, but far less information is available regarding adult patients with NHL, and few studies have considered genetic factors as covariate effects. Moreover, ethnicity is one factor that might account for the observed differences in both the pharmacokinetics (PK) and pharmacodynamics (PD) of drugs, which has resulted in variability in the responses to drug therapy [20]. Few PPK studies on MTX have provided pharmacogenetic information for non-Chinese patients, but the results have been controversial [21–23]. To the best of our knowledge, none of the published studies have established the PPK of HD-MTX in Chinese adult patients with NHL using a method that integrates genetic covariates.

We would like to concentrate on the genes mentioned above that have been demonstrated to affect the clinical outcome of MTX but whose impact on the PPK of MTX is inconclusive or unknown. Therefore, the following candidate genetic variants were selected for the present study: rs10106 in *FPGS*; rs719235, rs10464903 and rs12681874 in *GGH*; rs4149056 and rs11045879 in *SLCO1B1*; rs1045642 in *ABCB1*; and rs1801131 and rs1801133 in *MTHFR*.

In clinical practice, the routine monitoring of MTX concentrations includes several blood samplings. Patients with MTX concentrations at 72 h that remain above the rescue threshold (0.2  $\mu\text{mol/L}$ ) should stay longer in the hospital for additional hydration and leucovorin rescue. A new sampling strategy involves fewer samples than those used in routine practice. The early prediction of increased MTX concentrations at 72 h based on this new sampling strategy reduces the number of samples and the hospital duration.

This study aimed to identify physiological and pharmacogenomic covariates that can explain the inter- and intraindividual pharmacokinetic variability of MTX in Chinese adults with NHL and to explore a new sampling strategy for predicting delayed MTX elimination.

## Materials and methods

### Patients and study design

The study involved adult patients (age  $\geq 18$  years) who were diagnosed with NHL and treated with HD-MTX at Fujian Cancer Hospital from July 2013 to December 2018. Patients with diffuse large B-cell lymphoma were treated with MTX  $\pm$  cytarabine [24, 25]. The NHL–Berlin–Frankfurt–Münster 95 protocol (NHL–BFM95) and ALL–Berlin–Frankfurt–Münster 95 protocol (ALL–BFM95) were used for the treatment of Burkitt’s and T-lymphoblastic lymphoma [26, 27], respectively, whereas the AspaMet-Dex protocol was used for the treatment of NK/T-cell lymphoma [28].

The administration of HD-MTX at 1–3 g/m<sup>2</sup> was followed by leucovorin rescue, which was administered 36 h after initiation of the MTX infusion and repeated every 6 h until the MTX concentration decreased to less than 0.2  $\mu\text{mol/L}$  [29].

Intravenous hydration and alkalization were achieved 12 h prior to the start of MTX therapy to provide protection against MTX-induced renal dysfunction [4]. MTX concentration monitoring was performed until the MTX plasma concentration was below 0.2  $\mu\text{mol/L}$ . The study was approved by the ethics committee of Fujian Cancer Hospital. Informed consent was obtained from the patients and/or guardians.

### Analytical method

The plasma was separated by centrifugation at 3500 g for 5 min, and the separated plasma samples were used for analysis. The MTX concentrations were measured by high-performance liquid chromatography (HPLC), and the chromatographic system consisted of a Beckman-C18 (150 mm  $\times$  4.6 mm, 5  $\mu\text{m}$ ) analytical column with a mobile phase of 40 mM sodium acetate buffer (pH 4.6):acetonitrile (88.9:11.1, v/v) and ultraviolet detection at 294 nm. The flow rate of the mobile phase was maintained at 1.0 mL/min. The injection volume was 20  $\mu\text{L}$  with a run time of 6 min. The method was linear within the range of 0.09–3.52  $\mu\text{mol/L}$ , and the intra- and interday precision was < 6%. The limit of quantification (LOQ) was 0.09  $\mu\text{mol/L}$ .

### Genotyping

Genomic DNA was isolated from whole blood using the Qiagen DNA Blood Mini Kit (Qiagen, CA, USA) following the manufacturer’s instructions. The DNA purity and concentration were checked by spectrophotometric measurement of the absorbance at 260 and 280 nm.

Genotyping for rs10106, rs719235, rs10464903, rs12681874, rs4149056, rs11045879, rs1045642, rs1801131, and rs1801133 was performed using the Sequenom MassARRAY technology platform with the complete iPLEX Gold Reagent Set (Sequenom, CA, USA) by the Beijing Genomics Institute Genomics Company (Beijing, China). Allele detection was performed by matrix-assisted laser desorption/ionization time-of-flight mass spectrometry. The assay data were analyzed using Sequenom TYPER software (version 4.0). The primers were designed by ADS software 2.0 (Agena Bioscience, CA, USA).

### Base model

The pharmacokinetic analysis was conducted by nonlinear mixed-effects modeling using NONMEM<sup>®</sup> Version 7.4.1 (ICON Development Solutions, Hanover, MD, USA). The first-order conditional estimate method with eta-epsilon interaction (FOCE-I) was used throughout the model-building process. The tools used to evaluate and visualize the model were R Version 3.4.1 (R Foundation for Statistical Computing, Vienna, Austria) and PsN Version 4.6.0 (<https://uopharmacometrics.github.io/PsN/>), which are all within the graphical interface Pirana Version 2.9.7 (Certara, St. Louis, MO, USA) [30].

Two- and three-compartment models were investigated to describe the concentration–time data based on a literature review and visual data inspection.

The interindividual variability (IIV) of the PK parameters was evaluated using the exponential model shown in Equation (Eq. 1):

$$P_{ij} = TV(P) \cdot e^{\eta_i + k_{ij}}, \quad (1)$$

where  $P_{ij}$  is the parameter estimate for the  $i$ th individual on the  $j$ th occasion and  $TV(P)$  is a typical value for the parameter. The difference between logarithms of  $P_{ij}$  and  $TV(P)$  is described by  $\eta_i$ , and  $k_{ij}$  is the interoccasion variability (IOV) used to represent the random difference of occasion  $j$  from the individual  $i$  average value.

Additive (Eq. 2), proportional (Eq. 3) and combination error models (Eq. 4) were evaluated to describe the residual variability.

$$Y = F + \text{EPS}(1) \quad (2)$$

$$Y = F + F \times \text{EPS}(2) \quad (3)$$

$$Y = F + F \times \text{EPS}(2) + \text{EPS}(1), \quad (4)$$

where  $Y$  is the observed MTX concentration,  $F$  is the model-predicted concentration, and  $\text{EPS}(1)$  and  $\text{EPS}(2)$  represent the residual error of the model with a means of 0 and variances of  $\sigma_1^2$  and  $\sigma_2^2$ , respectively.

Model selection was based on the Akaike information criterion (AIC), Bayesian information criterion (BIC), objective function value (OFV), parameter precision, shrinkage values, and visual inspection of the corresponding goodness-of-fit plots. A shrinkage value below 20% was considered acceptable [31].

## Covariate analysis

Once the base model was selected, covariates were tested for their influence on pharmacokinetic parameters. The covariates tested were age, sex, height, body weight, body surface area (BSA), disease stage, hematocrit, serum creatinine (SCR), blood urea nitrogen (BUN), creatinine clearance (CrCL), alanine aminotransferase (ALT), aspartate aminotransferase (AST), albumin and SNPs of *FPGS*, *GGH*, *SLCO1B1*, *ABCB1*, and *MTHFR*. CrCL was estimated using the Chronic Kidney Disease Epidemiology Collaboration 2009Scr (CKD-EPI2009Scr) equation [32].

The influence of the continuous covariate (CO) of each patient was modeled using the following linear (Eq. 5), power (Eq. 6), and exponential (Eq. 7) equations:

$$P_i = TV(P) + \theta \times (CO_i/CO_{\text{median}}) \quad (5)$$

$$P_i = TV(P) \times (CO_i/CO_{\text{median}})^\theta \quad (6)$$

$$P_i = TV(P) \times e^{(\theta \times CO_i/CO_{\text{median}})}, \quad (7)$$

where  $P_i$  is the value of  $P$  for the  $i$ th individual,  $TV(P)$  is the typical value of parameter  $P$ ,  $CO_i$  is the covariate of the  $i$ th individual,  $CO_{\text{median}}$  is the median value of the covariate, and  $\theta$  is the coefficient term to be estimated.

The effect of categorical covariates on parameter  $P$  was tested according to (Eq. 8), which uses sex as an example.

$$\begin{aligned} P_i &= TV(P)_{\text{sex} = \text{male}} \\ P_i &= TV(P) \times \theta_{\text{sex} = \text{female}} \end{aligned} \quad (8)$$

The influence of the SNPs on parameter  $P$  was evaluated by additive, recessive, and dominant genetic models using the following equation:

$$P_i = TV(P) + \theta \times \text{geno} \quad (9)$$

The SNPs were classified as homozygous wild-type (wt), heterozygous (het), and homozygous variant (var) genotypes. For the additive model,  $\text{geno} = 0, 1$  or  $2$  for the wt, het, and var genotypes, respectively. For the recessive model,  $\text{geno} = 0$  for both the wt and het genotypes, and  $\text{geno} = 1$  for the var genotype. For the dominant model,  $\text{geno} = 0$  for the wt genotype, and  $\text{geno} = 1$  for both het and var genotypes. In addition,  $\theta$  is the estimated covariate effect.

A forward inclusion and backward elimination approach was used to evaluate the statistical significance of relevant covariates. Covariates that decreased the OFV by more than 3.84 ( $p < 0.05$ ) were added to the full model. Backward elimination was then performed with a stricter statistical significance of  $p < 0.01$  ( $\text{OFV} > 6.64$ ). An additional criterion for the inclusion of covariates in the final model was that the impacts of the covariates be biologically reasonable.

## Model validation

The goodness of fit of the final model was evaluated by checking the plots of the observed concentrations versus the population- or individual predicted concentrations and the conditional-weighted residuals versus the population-predicted concentrations or time. Two procedures were used to evaluate the stability and predictive ability of the final model. First, a bootstrap resampling method was applied [33]. One thousand bootstrap datasets were generated by sampling randomly from the original dataset with replacement, and the medians of the parameters of the bootstrap dataset were then compared to the estimates of the original dataset. The model was further validated by the prediction-corrected visual predictive check (PC-VPC) based on 1000 simulated datasets [34]. The median and 95% confidence intervals (CI) of the simulated predictions were compared to the observed data.

## Model application

The changes in the percentages of patients with renal dysfunction who had MTX concentrations below  $0.2 \mu\text{mol/L}$  at 72 h were analyzed using six scenarios based on the administration of 1, 2, and  $3 \text{ g/m}^2$  to patients with the same BSA ( $1.65 \text{ m}^2$ ) but different renal functions ( $\text{CrCL} = 60$  or  $90 \text{ ml/min/1.73 m}^2$ ). Plasma MTX concentration–time profiles were simulated for 1000 hypothetical patients in each scenario based on the final population PK model.

## New sampling strategy

To identify suitable sampling strategies for forecasting the concentration at 72 h, the impact of prior observed concentrations on model predictability was assessed by maximum a posteriori Bayesian forecasting using a validation dataset. The individual prediction (IPRED) of the concentration at 72 h was estimated based on one prior observation (MTX concentration at 24, 36, 42 and 48 h, respectively) and two prior observations (MTX concentrations at 24–36 h, 24–42 h, 24–48 h, 36–42 h and 36–48 h). The comparison of the observed concentration to that estimated using the Bayesian approach at 72 h was denoted by the individual prediction error [IPE%]. The median individual prediction

error (MPE%), the root median squared relative individual prediction error (RMSE%), the percentage of IPEI% within 20% (IF20) and IF30 were used to evaluate the accuracy and precision of the predictability with different prior information.

## Results

### Patient characteristics

A total of 852 MTX concentrations from 91 patients with NHL were available for model building. Of the patients, 70.3% were males, and 12.1% were older than 65 years. Twenty-one of these patients had renal dysfunction (CrCL < 90 mL/min/1.73 m<sup>2</sup>). Eighteen patients with 196 observations were included in the validation dataset. The demographic and clinical characteristics of the patients included in the modeling and validation datasets are presented in Table 1.

### Genotyping

Six SNPs in three genes encoding enzymes of the folate metabolic pathway (FPGS, GGH, and MTHFR) and three SNPs in two MTX transporter genes (*SLCO1B1* and *ABCB1*) were

analyzed. All genotype groups were in Hardy–Weinberg equilibrium. The genotypes of the targeted SNPs and the associated Hardy–Weinberg equilibrium results are shown in Table 2.

### Base model

The data were best described by a two-compartment model according to the OFV, AIC, BIC, shrinkage values, and diagnostic plots. The inclusion of the IIV on the clearance (CL), the intercompartmental clearance (Q), and the volume of the central compartment (V1) significantly improved the model, and the OFV decreased further after the introduction of the IOV on the CL. The residual variability was described by a proportional error model.

### Covariate analysis

Covariate analysis performed by forward inclusion into the base model indicated that the CL was affected by CrCL ( $\Delta\text{OFV} = 17.1$ ,  $p < 0.001$ ). After inclusion of the CrCL on the CL, only the BSA could be added on the Q. After backward exclusion, the final model that included the effect of the CrCL on the CL and that of the BSA on the Q was obtained ( $\Delta\text{OFV} = 24.766$ ,  $p < 0.001$ ).

None of the genotypes exerted a significant effect on MTX CL or V1, and the relationship among the CL, V1 and the target SNPs is shown in Fig. 1.

The final PK model for MTX in Chinese adult patients with NHL was as follows:

$$\text{CL} \left( \frac{L}{h} \right) = 6.03 \times \left( \frac{\text{CrCL}}{115.1} \right)^{0.414} \quad (10)$$

**Table 1** Patient characteristics

Characteristic	Median (range) or N	
	Modeling dataset	Validation dataset
Age (years)	48 (18–73)	42 (18–68)
Sex (male/female)	64/27	12/6
Height (cm)	164 (149–183)	160 (147–180)
Body weight (kg)	61 (44–90)	55.5 (36.5–78)
Body surface area (m <sup>2</sup> )	1.65 (1.28–2.06)	1.61 (1.35–1.98)
Pathology		
Diffuse large B-cell lymphoma	54	10
Burkitt's lymphoma	7	2
T-lymphoblastic lymphoma	11	3
NK/T-cell lymphoma	19	3
Disease stage (I–II/III–IV)	42/49	8/10
Hematocrit (%)	35.55 (16–48)	34.2 (23.3–41.6)
Serum creatinine (μmol/L)	72 (32–113)	68 (40–108)
Blood urea nitrogen (mmol/L)	4.28 (1.63–9.27)	4.35 (2.78–8.48)
CrCL (mL/min/1.73 m <sup>2</sup> )	115.1 (60–153.4)	108.3 (70.2–140.5)
Alanine transaminase (IU/L)	20 (2–110)	23.5 (8–107)
Aspartate transaminase (IU/L)	21 (11–72)	19.5 (11–77)
Albumin (g/L)	37.9 (21.5–50)	37 (20.7–46)

**Table 2** Genotype of the targeted SNPs

Gene	Rs no	Genotype frequency (n/%)			p*
		wt	het	var	
<i>FPGS</i>	rs10106	47 (51.65)	35 (38.46)	9 (9.89)	0.515
	rs719235	70 (76.92)	19 (20.88)	2 (2.20)	0.604
<i>GGH</i>	rs10464903	35 (38.46)	44 (48.35)	12 (13.19)	0.753
	rs12681874	39 (42.86)	41 (45.05)	11 (12.09)	0.964
<i>SLCO1B1</i>	rs4149056	75 (82.42)	14 (15.38)	2 (2.20)	0.192
	rs11045879	27 (29.67)	48 (52.75)	16 (17.58)	0.501
<i>ABCB1</i>	rs1045642	41 (45.05)	38 (41.76)	12 (13.19)	0.502
<i>MTHFR</i>	rs1801131	59 (64.84)	30 (32.97)	2 (2.19)	0.417
	rs1801133	52 (57.14)	31 (34.07)	8 (8.79)	0.291

wt homozygous wild-type genotype, het heterozygous variant genotype, var homozygous variant genotype

\*Hardy–Weinberg equilibrium

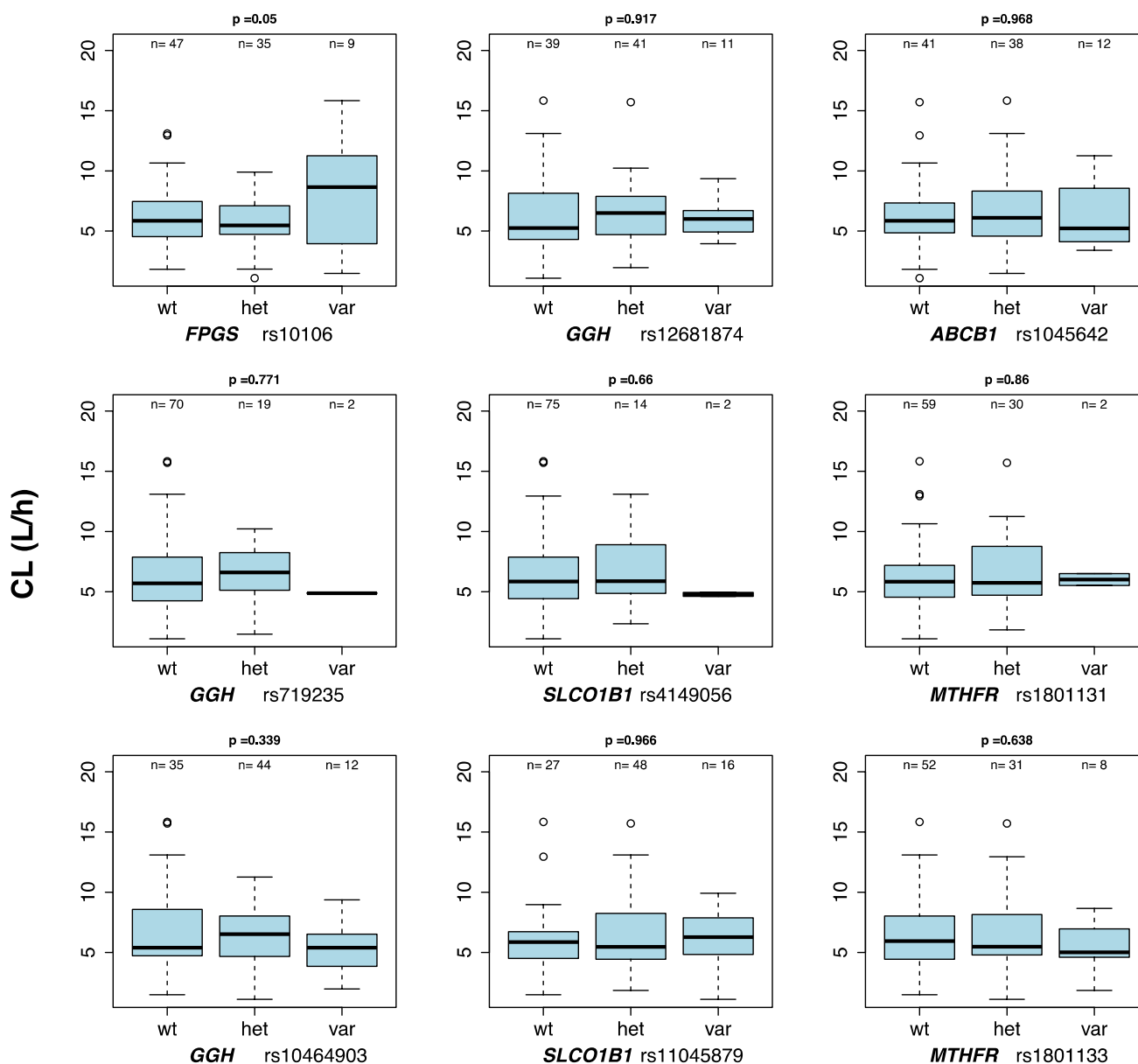


**Fig. 1** Relationship among CL, VI and the target SNPs

$$Q\left(\frac{L}{h}\right) = 0.074 \times \left(\frac{BSA}{1.65}\right)^{1.43} \quad (11)$$

### Model validation

The goodness-of-fit plots of the observations versus population and individual predictions obtained with the final model were densely distributed around the line of identity, and the conditional-weighted residuals were normally distributed, which indicated that the model adequately described the observed concentrations (Fig. 2).

The bootstrap analysis was successful in 86% of the 1000 runs, and the median parameter values as well as the 2.5% and 97.5% percentiles agreed with the final model estimations and errors, which indicated the stability of the final model (Table 3).

The PC-VPC, which exhibited an acceptable overlap of the 5th, 50<sup>th</sup>, and 95th percentiles of the observed data and the 95% CI of the corresponding simulations indicated the good predictive performance of the final model (Fig. 3).

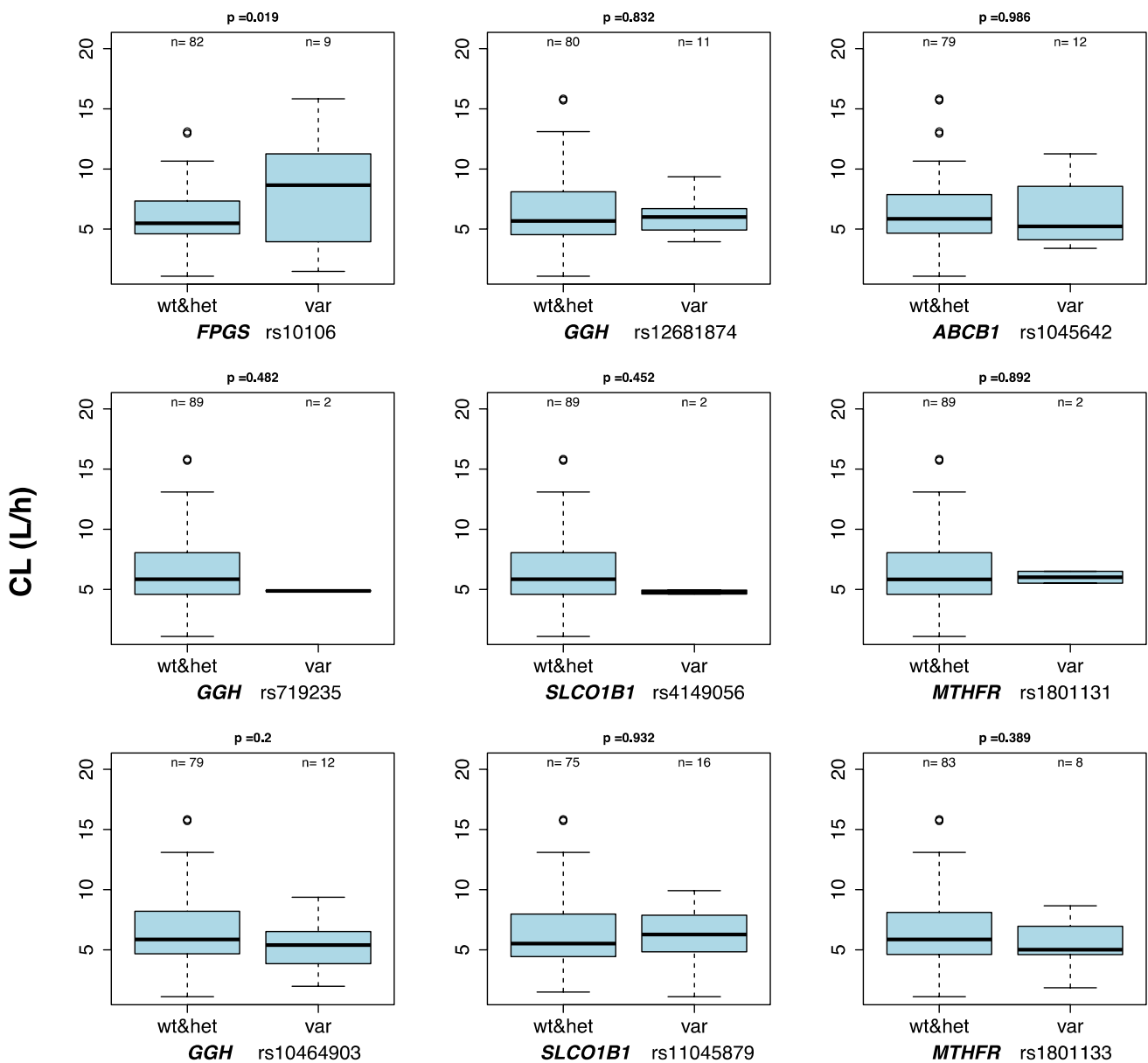


Fig. 1 (continued)

### Model application

The population medians of the simulated plasma concentration-versus-time profiles are shown in Fig. 4. The percentage of patients with concentrations below 0.2  $\mu\text{mol/L}$  at 72 h was dependent on the CrCL and related to the dose.

The percentage decreased from 65.6 to 42.6% when the CrCL decreased from 90 to 60 ml/min/1.73  $\text{m}^2$  with the scheduled dosing of 3  $\text{g/m}^2$ , and the same trend was obtained with dose regimens of 1 and 2  $\text{g/m}^2$ .

### New sampling strategy

Bayesian forecasting demonstrated that prior information could improve the prediction accuracy for the concentration at 72 h. Among the prior information groups, the one that included the MTX concentration at 36 h provided the best estimation of the concentration at 72 h, whereas prior information of the MTX concentration at 24 and 42 h provided the best estimation among all the tested groups (MPE% = -3.47%, RMSE% 12.76%, IF20 = 66.67%, IF30 = 80.56%).

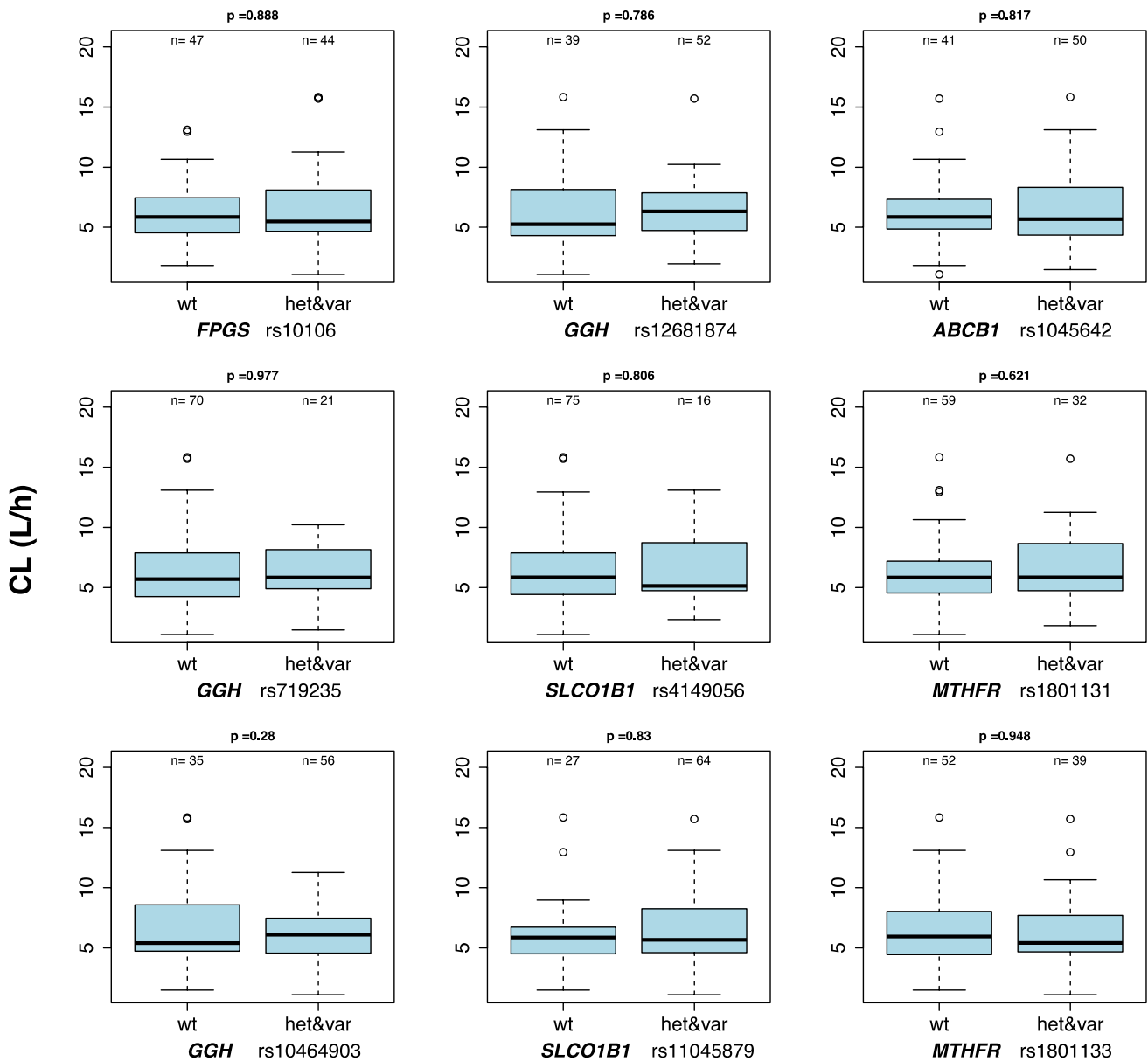


Fig. 1 (continued)

Boxplots of the individual prediction errors obtained with different prior information are presented in Fig. 5.

## Discussion

This study provides the first reported PPK model of MTX in Chinese adult patients with NHL that involves genetic factors as covariate effects. Our results show that the CrCL significantly influenced the CL and that the BSA was associated with the Q, but none of the target SNPs exerted a significant effect on the CL or V1.

Growing evidence suggests that polymorphisms in genes encoding transporters or enzymes might partly account for the MTX-PK variability. A study of European children and adolescents with lymphoblastic leukemia and malignant lymphoma screened *ABCB1* rs1045642, *MTHFR* rs1801131, and *MTHFR* rs1801133 and found that only *MTHFR* rs1801133 exhibited a significant effect on the MTX pharmacokinetics. The MTX CL in patients homozygous for the variant allele of *MTHFR* rs1801133 was 26% lower than that in homozygous wild-type individuals [21]. However, Kim et al. [22] found a significant association between *ABCB1* rs1045642, but not *MTHFR* rs1801133 and the MTX CL. Their study included 20 Korean patients treated with



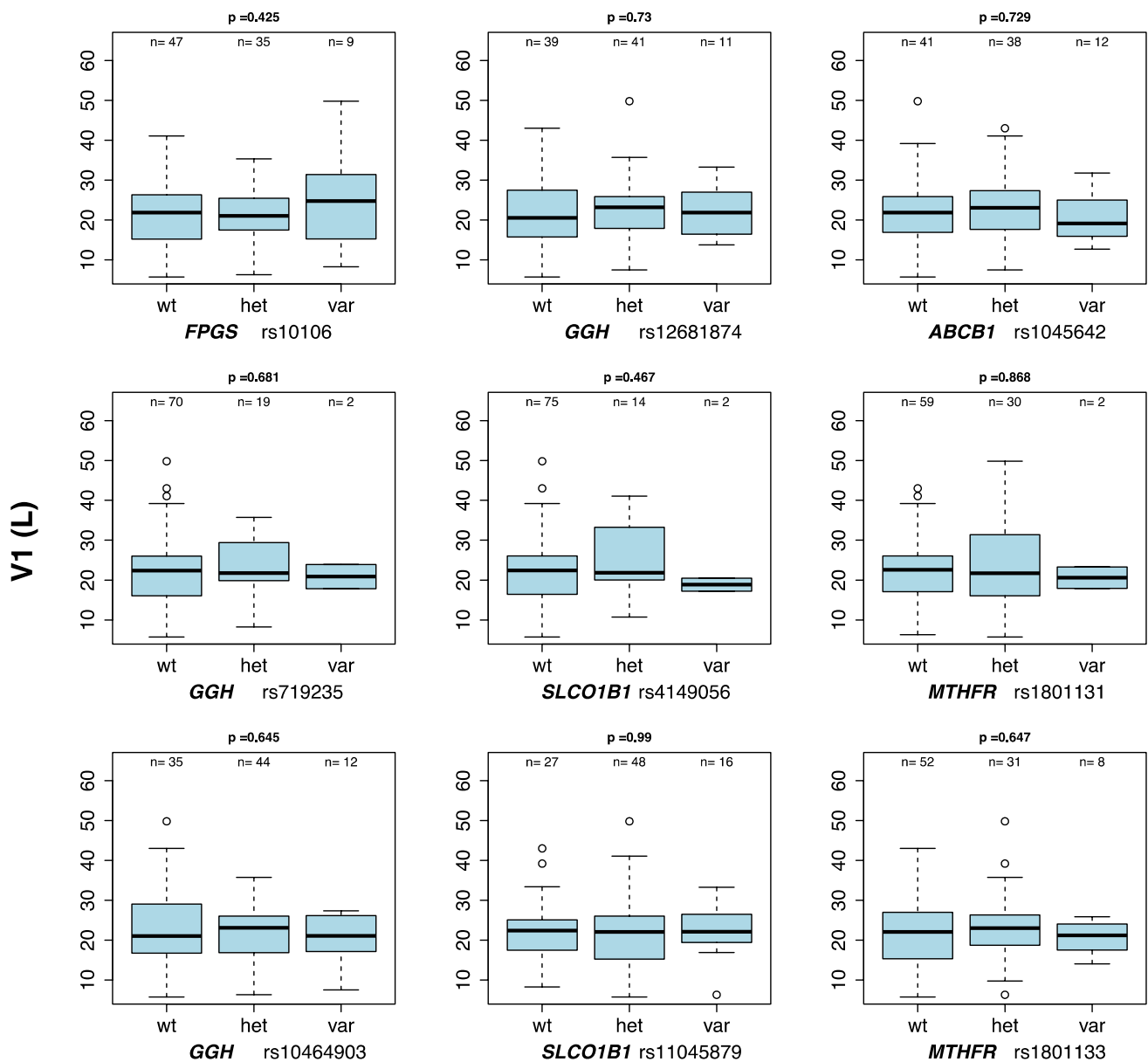


Fig. 1 (continued)

low-dose MTX (10–15 mg/kg) after hematopoietic stem cell transplantation.

A large cohort and genome-wide association study showed that the *SLCO1B1* genotypes were significant predictors of the  $AUC_{0-48\text{ h}}$  of MTX and significantly associated with the  $C_{24\text{ h}}$  and clearance of MTX [11]. Although OATP1B1 is not expressed in the kidney, SNPs of *SLCO1B1* might interfere with renal transporters responsible for MTX elimination in urine by affecting the accumulation of endogenous metabolites in blood, which are subsequently excreted in urine [35]. Gabrielle et al. [23] evaluated the influence of 54 SNPs located in the *SLCO1B1*, *ABCB1*, *ABCC1*, *ABCC2*, *ABCC3*, *ABCC4*, *ABCG2*, *SLC19A1*, and *UGT1A1* genes

on the MTX PPK model for 187 osteosarcoma patients; in the patient cohort, *SLCO1B1* was the most significant. Woillard et al. [36] developed a three-parameter time-dependent MTX PPK model that accounted for the nonlinearity in the clearance using Pmetrics and found that the time-dependent model might be better than a previously published two-compartment model developed using NONMEM.

In the present study, we analyzed nine SNPs in *FPGS*, *GGH*, *SLCO1B1*, *ABCB1*, and *MTHFR* as covariates, and none of the genotypes exerted a significant effect on the MTX pharmacokinetic properties. The main MTX elimination route might vary among treatment protocols used for different types of cancer [23], which might partly account for

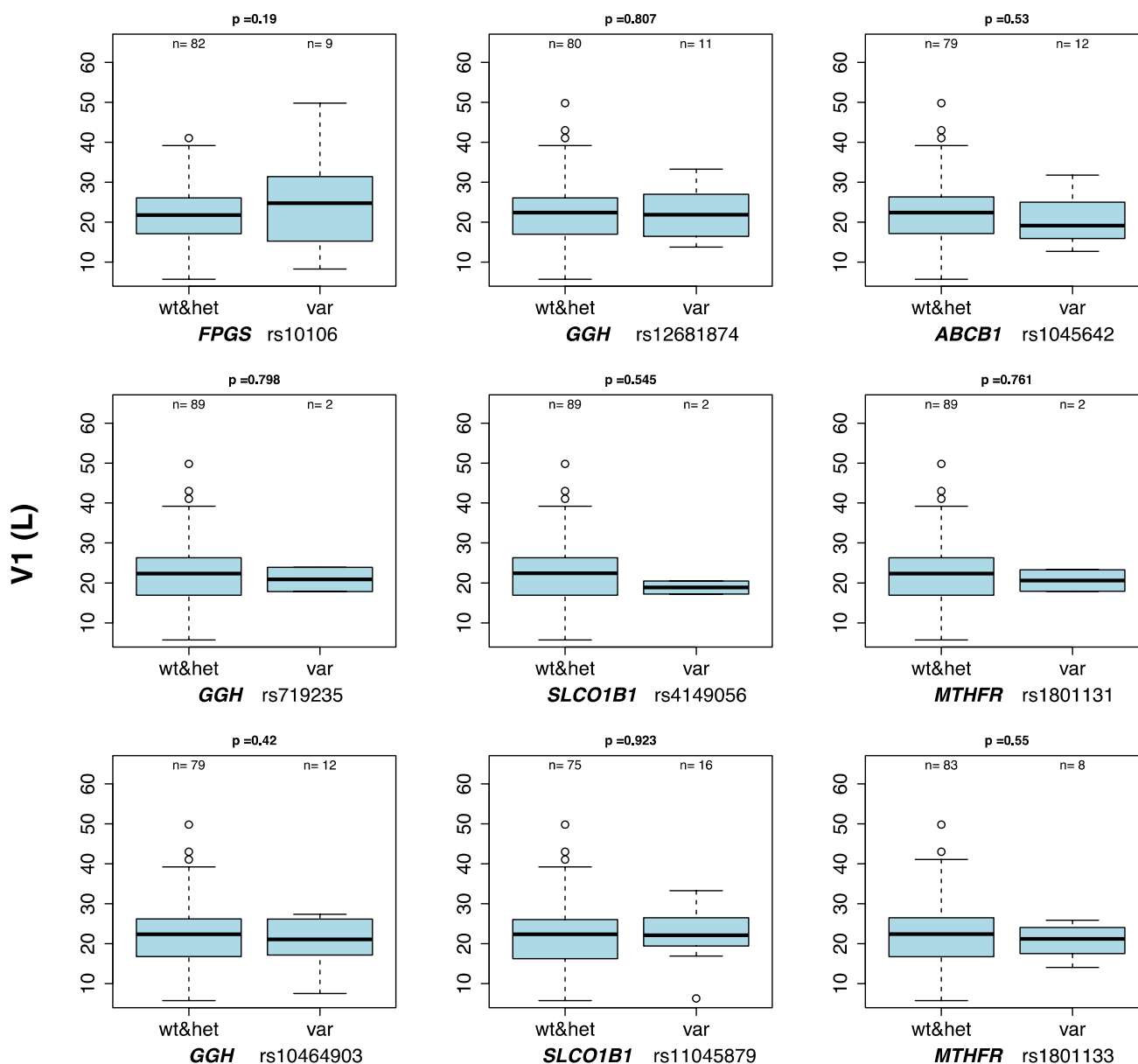


Fig. 1 (continued)

the above-mentioned inconformity. Furthermore, the present study might not have sufficient power to detect a significant association between the targeted SNPs and the MTX pharmacokinetic properties.

In our final PPK model, the typical values of CL (6.03 L/h) and V1 (20.7 L) were comparable to the values reported by Faltaos et al. [37] (CL, 7.1 L/h; V1, 25.1 L), Kotnik et al. [21] (CL, 7.43 L/h; V1, 16.7 L), and Mei et al. [38] (CL, 6.67 L/h; V1, 24.5 L).

Some studies have reported that the MTX CL is influenced by the CrCL [29, 39, 40]. Our study showed that incorporation of the CrCL for prediction of the MTX CL led to a decrease in the OFV by 17.1 points ( $p < 0.001$ ).

We also found that a decrease in CrCL corresponded to a lower body weight-normalized CL in both men and women (Fig. 6). The significant influence of CrCL on MTX CL could be explained by the fact that renal excretion is the predominant MTX elimination route.

We found an IOV on CL, which suggested that elimination parameters might vary across MTX courses. The IOV on CL was estimated to equal 15.4%, in agreement with previous PPK reports (14.8% and 16.6%, respectively) [21, 23].

We also found that BSA was a significant covariate in Q, which was similar to the results obtained in two previous studies [38, 39]. Although both body weight and hematocrit exerted a significant effect on methotrexate CL and V1

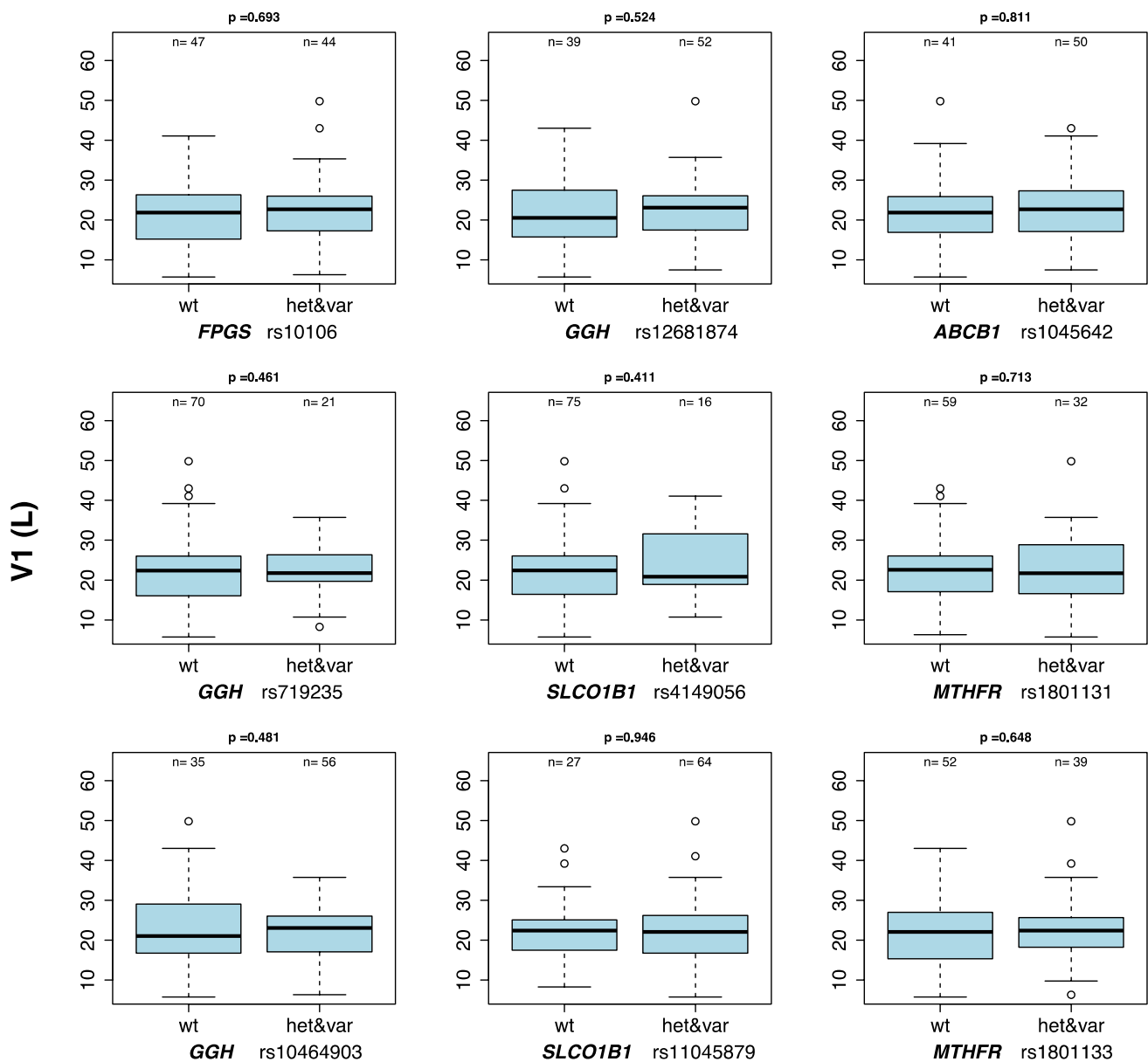


Fig. 1 (continued)

in some published models [41–43], no significant results were observed in the present study, which was similar to the results reported by Mei et al. [38].

Patients with high doses and renal dysfunction are at higher risk of delayed elimination. The time it took for the MTX concentration to decrease below the rescue threshold (0.2  $\mu\text{mol/L}$ ) exhibited a wide variability between groups with different renal functions or different doses, as shown in Fig. 4, which suggests that MTX monitoring should remain an important strategy for providing information regarding the elimination of MTX.

A study performed in children with ALL showed that Bayesian estimation using a one-sample (48 h) schedule

yielded better results for predicting delayed elimination to reach a concentration less than 0.2  $\mu\text{mol/L}$  compared with a two-sample schedule (24 and 48 h) [44]. However, Christine et al. [45] tested a one-sample schedule (each of the available blood samples) and a two-sample schedule (five combinations) and demonstrated that two sampling times (24 and 48 h) allowed more precise and accurate determination of individual pharmacokinetic parameters. In the present study, the two-sample schedule (24 and 42 h) showed the most accurate and precise prediction of the concentration at 72 h.

This study has some limitations. First, the sample size was relatively small (852 observations from 91

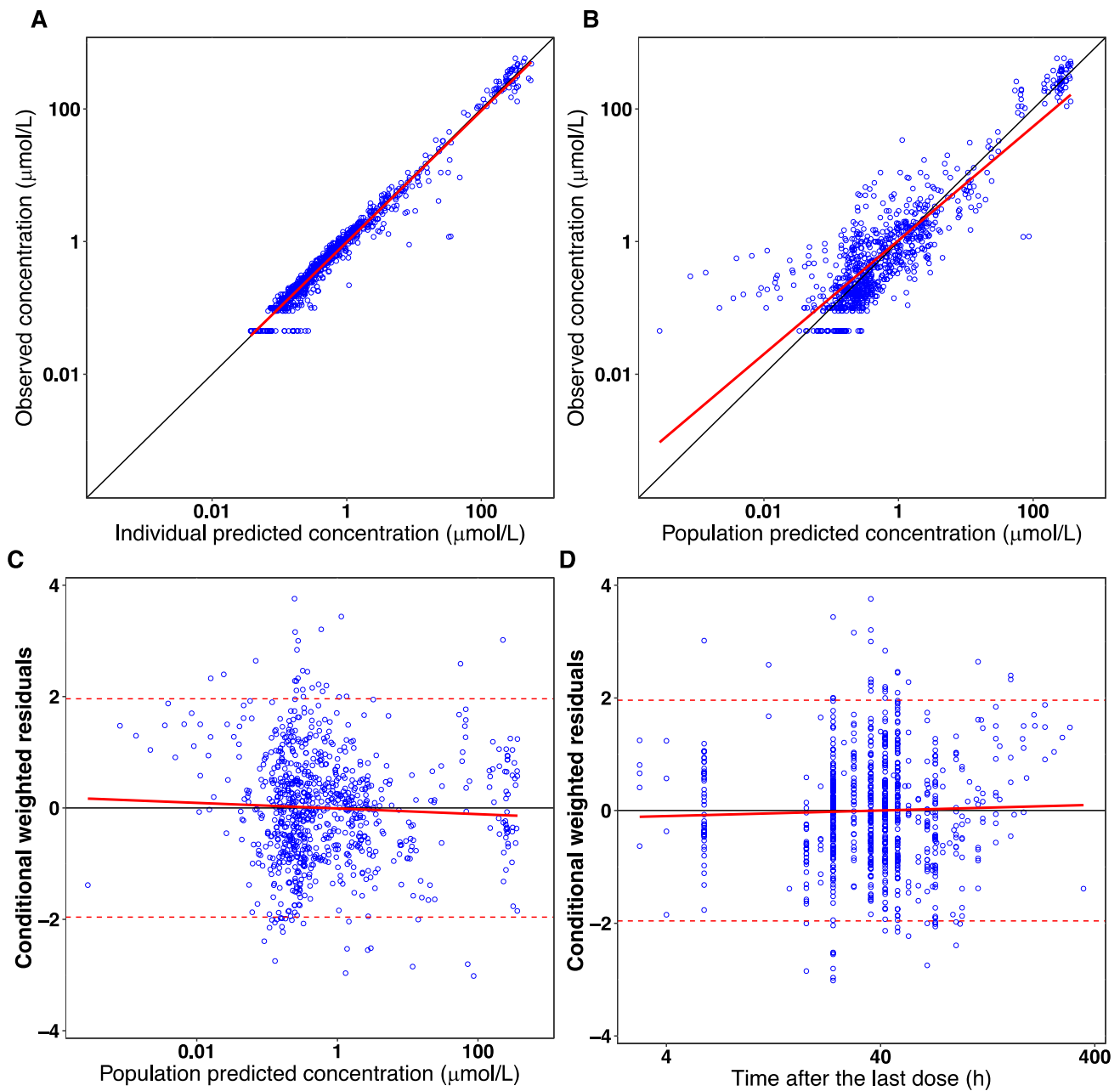


**Fig. 2** Goodness-of-fit plots of the final model. **a** Observed concentration vs. individual-predicted concentration, **b** observed concentration vs. population-predicted concentration (PRED), **c** conditional-

weighted residuals (CWRES) vs. PRED, and **d** CWRES vs. time after the last dose. The solid lines in **a** and **b** are identity lines, and the solid lines in **c** and **d** are zero lines. The Y-axis is on a log scale

patients). Second, some important SNPs, such as *SLC19A1* rs1051266, *ABCB1* rs1128503, *ABCC1* rs28364006, *ABCC2* rs3740065, *ABCG2* rs2231142, and *ABCG2* rs13120400, were not identified in this study but will be taken into consideration in our future studies. Third, the present study relied on routine MTX monitoring data, which did not include concentrations of MTX in urine or concentrations of MTX metabolites.

## Conclusion

An MTX population pharmacokinetic model for Chinese adult patients with NHL was developed and validated. Lower CrCL resulted in lower MTX CL, and the BSA was positively correlated with Q. It is important to assess the renal function in each patient prior to the initiation of chemotherapy, and to pay attention to the MTX accumulations in patients with a high BSA. None of the targeted

**Table 3** Population pharmacokinetic parameters of MTX

Parameter	Symbol	Final model estimate (RSE%)	Bootstrap median	2.5–97.5% percentile range
CL (L/h)	$\theta_1$	6.03 (9)	5.71	5.15–6.91
V1 (L)	$\theta_2$	20.70 (10)	19.68	16.94–24.48
Q (L/h)	$\theta_3$	0.074 (18)	0.069	0.050–0.098
V2 (L)	$\theta_4$	3.76 (25)	3.61	1.31–6.22
CrCL on CL	$\theta_5$	0.414 (23)	0.396	0.212–0.615
BSA on Q	$\theta_6$	1.43 (36)	1.49	0.269–2.58
Interindividual variability (%)				
CL	$\eta_1$	51.6 (14)	49.7	37.0–62.9
V1	$\eta_2$	48.3 (19)	44.3	22.8–64.4
Q	$\eta_3$	65.6 (13)	62.3	49.7–78.3
Interoccasion variability (%)				
CL	$k$	15.4 (12)	15.0	11.0–19.0
Residual error	$\epsilon$	0.319 (5)	0.321	0.285–0.352

RSE relative standard error

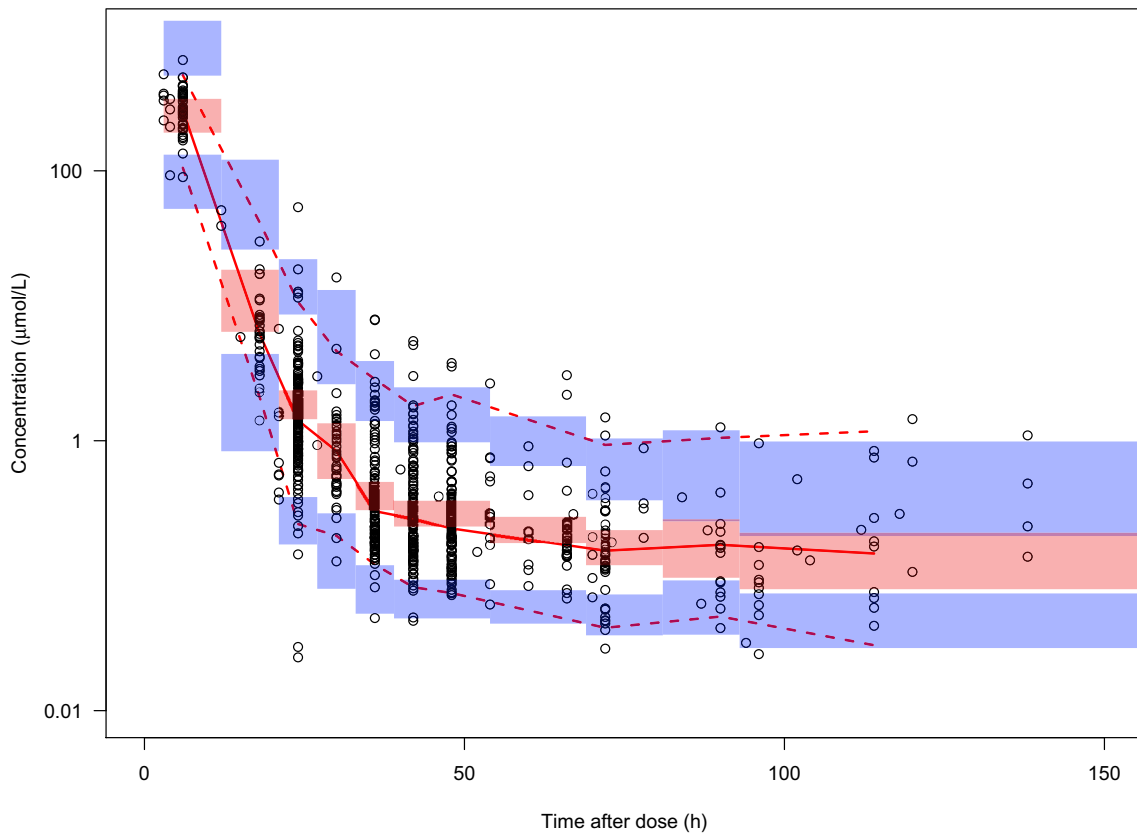


**Fig. 3** Prediction-corrected visual predictive check of the final model. The dots indicate the observed concentrations. The lines represent the 5th, 50th, and 95th percentiles of the observed data. The shaded areas are the 95% confidence intervals for the same percentiles of the simulations

SNPs in *FPGS*, *GGH*, *SLCO1B1*, *ABCB1* or *MTHFR* exerted a significant effect on the MTX pharmacokinetic properties. Model simulation quantified the differences

in reaching the threshold at 72 h between patients with different renal functions and doses. A schedule involving two samples, at 24 and 42 h, might be able to forecast

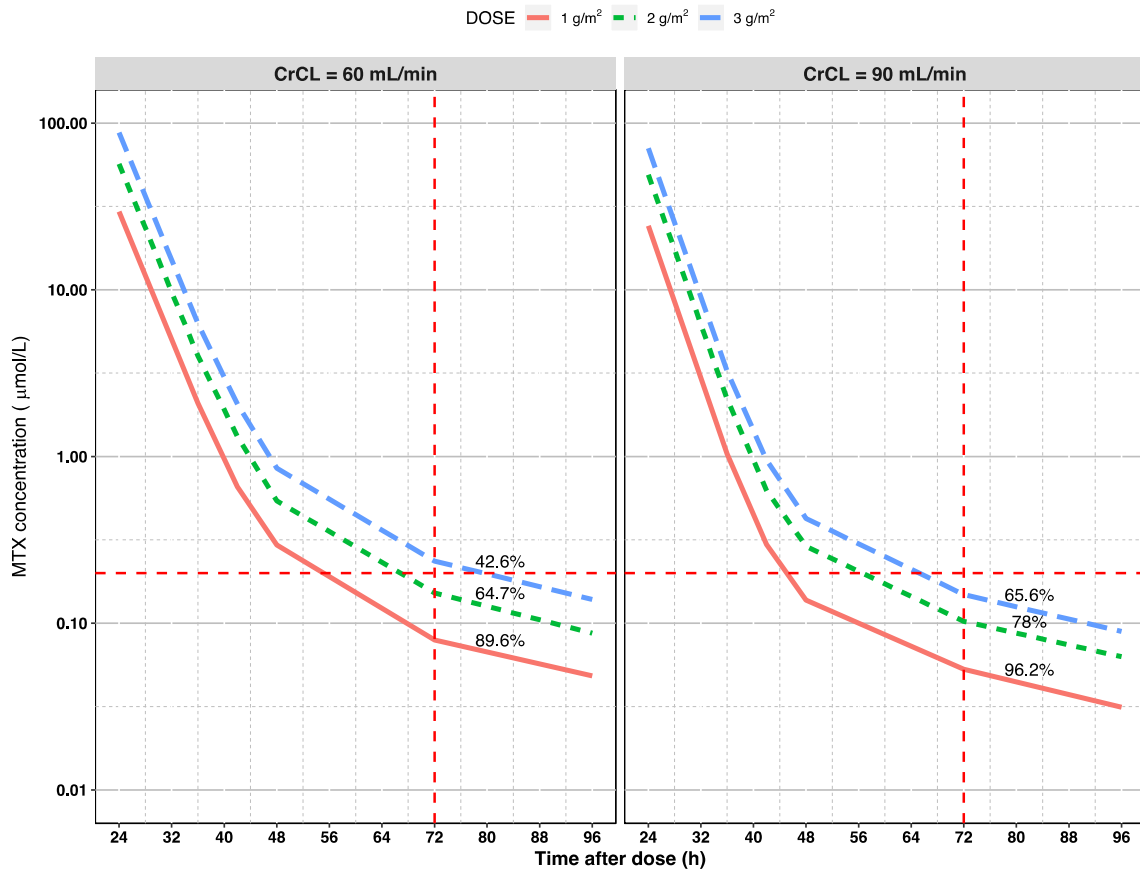


Fig. 4 Simulated plasma profiles of MTX under conditions involving different renal functions and dosages

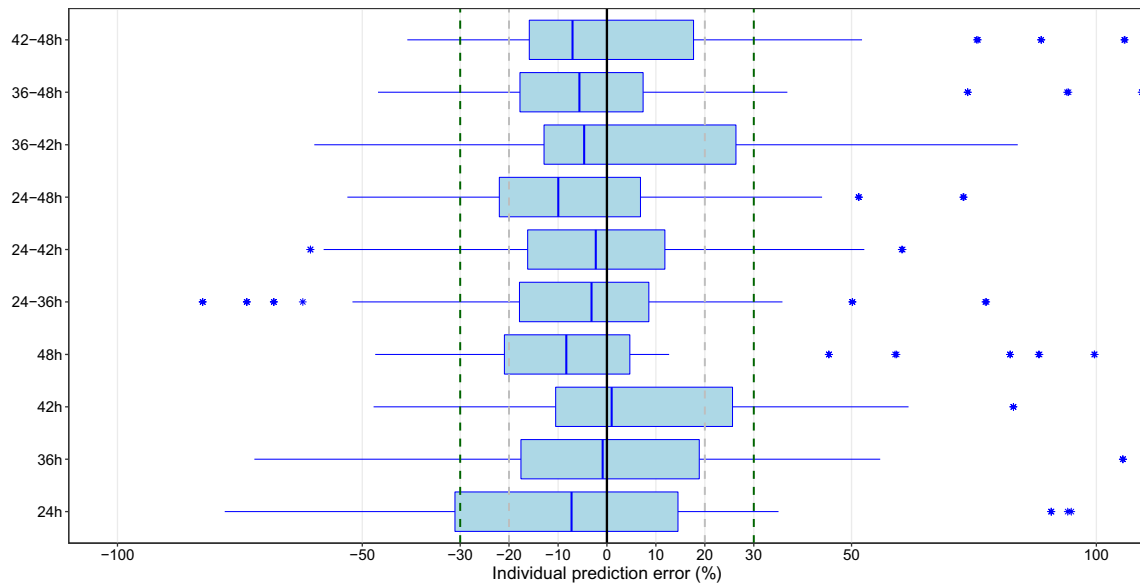
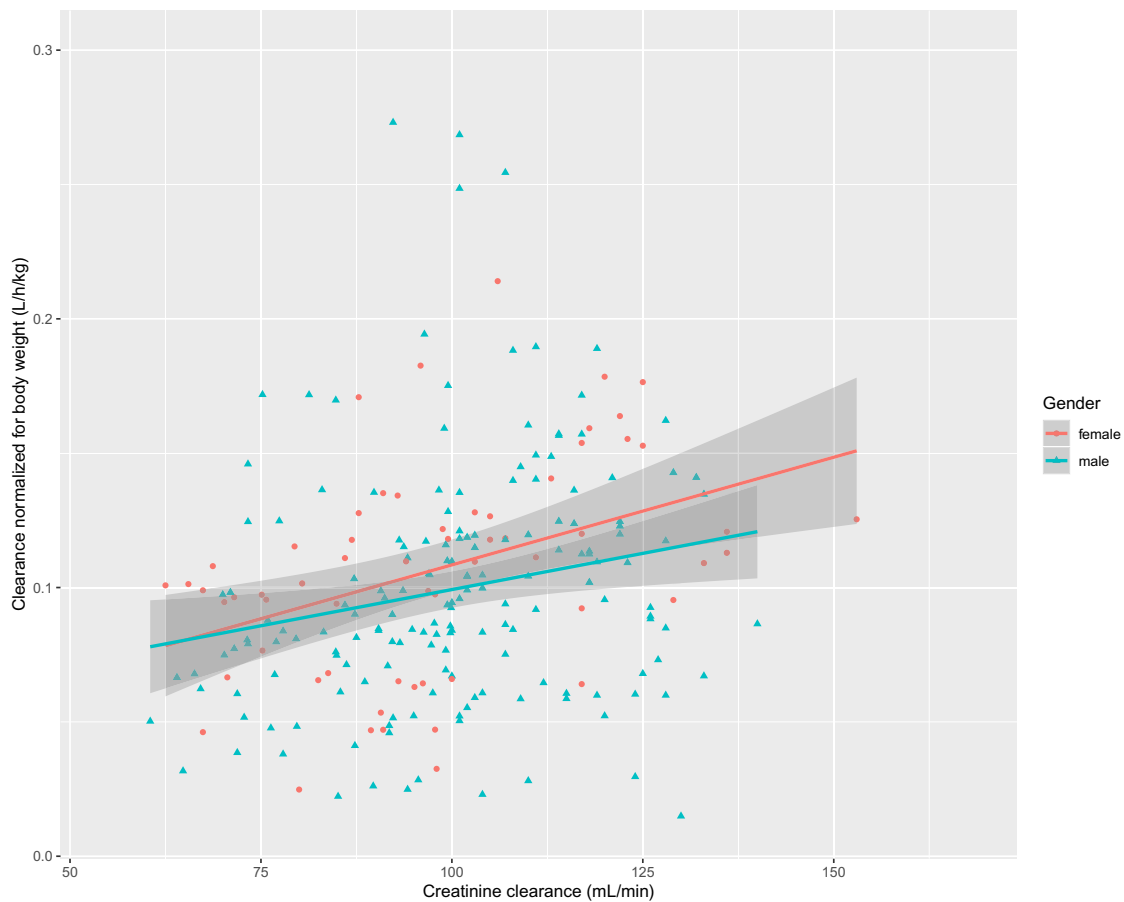


Fig. 5 Box plots of the individual prediction errors in different scenarios



**Fig. 6** Relationship between body weight-normalized clearance and creatinine clearance

delayed elimination, but this finding needs to be validated in a prospective study.

**Funding** This study was supported by the Fujian Provincial Health Technology Project (No: 2018-ZQN-18), the Natural Science Foundation of Fujian Province (No: 2016J01509), and the Science and Technology Program of Fujian Province, China (No: 2018Y2003).

### Compliance with ethical standards

**Conflict of interest** The authors declare that there are no conflict of interest.

### References

- Reiter A, Schrappe M, Tiemann M, Ludwig WD, Yakisan E, Zimmermann M, Mann G, Chott A, Ebell W, Klingebiel T, Graf N, Kremens B, Muller-Weihrich S, Pluss HJ, Zintl F, Henze G, Riehm H (1999) Improved treatment results in childhood B-cell neoplasms with tailored intensification of therapy: a report of the Berlin-Frankfurt-Munster Group Trial NHL-BFM 90. *Blood* 94(10):3294–3306
- Maia MB, Saivin S, Chatelut E, Malmarmy MF, Houin G (1996) In vitro and in vivo protein binding of methotrexate assessed by microdialysis. *Int J Clin Pharmacol Ther* 34(8):335–341
- Fotoohi AK, Albertioni F (2008) Mechanisms of antifolate resistance and methotrexate efficacy in leukemia cells. *Leuk Lymphoma* 49(3):410–426. <https://doi.org/10.1080/10428190701824569>
- Hospira (2017) Label for methotrexate injection. Lake Forest, IL; Hospira; 2011. [https://www.accessdata.fda.gov/drugsatfda\\_docs/label/2011/011719s1171bl.pdf](https://www.accessdata.fda.gov/drugsatfda_docs/label/2011/011719s1171bl.pdf). Accessed 29 Dec 2019
- Takatori R, Takahashi KA, Tokunaga D, Hojo T, Fujioka M, Asano T, Hirata T, Kawahito Y, Satomi Y, Nishino H, Tanaka T, Hirota Y, Kubo T (2006) ABCB1 C3435T polymorphism influences methotrexate sensitivity in rheumatoid arthritis patients. *Clin Exp Rheumatol* 24(5):546–554
- Trevino LR, Shimasaki N, Yang W, Panetta JC, Cheng C, Pei D, Chan D, Sparreboom A, Giacomini KM, Pui CH, Evans WE, Relling MV (2009) Germline genetic variation in an organic anion transporter polypeptide associated with methotrexate pharmacokinetics and clinical effects. *J Clin Oncol* 27(35):5972–5978. <https://doi.org/10.1200/JCO.2008.20.4156>
- Bleyer WA (1978) The clinical pharmacology of methotrexate: new applications of an old drug. *Cancer* 41(1):36–51
- Sterba J, Valik D, Bajciová V, Kadlecová V, Gregorová V, Mendelová D (2005) High-dose methotrexate and/or leucovorin rescue for the treatment of children with lymphoblastic malignancies: do we really know why, when and how? *Neoplasma* 52(6):456–463

9. Evans WE, Crom WR, Abromowitch M, Dodge R, Look AT, Bowman WP, George SL, Pui CH (1986) Clinical pharmacodynamics of high-dose methotrexate in acute lymphocytic leukemia. Identification of a relation between concentration and effect. *N Engl J Med* 314(8):471–477. <https://doi.org/10.1056/NEJM198602203140803>
10. Suthandiram S, Gan GG, Zain SM, Bee PC, Lian LH, Chang KM, Ong TC, Mohamed Z (2014) Effect of polymorphisms within methotrexate pathway genes on methotrexate toxicity and plasma levels in adults with hematological malignancies. *Pharmacogenomics* 15(11):1479–1494. <https://doi.org/10.2217/pgs.14.97>
11. Radtke S, Zolk O, Renner B, Paulides M, Zimmermann M, Moricke A, Stanulla M, Schrappe M, Langer T (2013) Germline genetic variations in methotrexate candidate genes are associated with pharmacokinetics, toxicity, and outcome in childhood acute lymphoblastic leukemia. *Blood* 121(26):5145–5153. <https://doi.org/10.1182/blood-2013-01-480335>
12. Chen Y, Shen Z (2015) Gene polymorphisms in the folate metabolism and their association with MTX-related adverse events in the treatment of ALL. *Tumour Biol* 36(7):4913–4921. <https://doi.org/10.1007/s13277-015-3602-0>
13. Lopez-Lopez E, Martin-Guerrero I, Ballesteros J, Garcia-Orad A (2013) A systematic review and meta-analysis of MTHFR polymorphisms in methotrexate toxicity prediction in pediatric acute lymphoblastic leukemia. *Pharmacogenomics J* 13(6):498–506. <https://doi.org/10.1038/tpj.2012.44>
14. Zhang HN, He XL, Wang C, Wang Y, Chen YJ, Li JX, Niu CH, Gao P (2014) Impact of SLCO1B1 521T %3e C variant on leucovorin rescue and risk of relapse in childhood acute lymphoblastic leukemia treated with high-dose methotrexate. *Pediatr Blood Cancer* 61(12):2203–2207. <https://doi.org/10.1002/pbc.25191>
15. Csordas K, Lautner-Csorba O, Semsei AF, Harnos A, Hegyi M, Erdelyi DJ, Eipel OT, Szalai C, Kovacs GT (2014) Associations of novel genetic variations in the folate-related and ARID5B genes with the pharmacokinetics and toxicity of high-dose methotrexate in paediatric acute lymphoblastic leukaemia. *Br J Haematol* 166(3):410–420. <https://doi.org/10.1111/bjh.12886>
16. Lima A, Bernardes M, Azevedo R, Monteiro J, Sousa H, Medeiros R, Seabra V (2014) SLC19A1, SLC46A1 and SLCO1B1 polymorphisms as predictors of methotrexate-related toxicity in Portuguese rheumatoid arthritis patients. *Toxicol Sci* 142(1):196–209. <https://doi.org/10.1093/toxsci/kfu162>
17. Avivi I, Zuckerman T, Krivoy N, Efrati E (2014) Genetic polymorphisms predicting methotrexate blood levels and toxicity in adult non-Hodgkin lymphoma. *Leuk Lymphoma* 55(3):565–570. <https://doi.org/10.3109/10428194.2013.789506>
18. Lopez-Lopez E, Martin-Guerrero I, Ballesteros J, Pinan MA, Garcia-Miguel P, Navajas A, Garcia-Orad A (2011) Polymorphisms of the SLCO1B1 gene predict methotrexate-related toxicity in childhood acute lymphoblastic leukemia. *Pediatr Blood Cancer* 57(4):612–619. <https://doi.org/10.1002/pbc.23074>
19. Li J, Wang XR, Zhai XW, Wang HS, Qian XW, Miao H, Zhu XH (2015) Association of SLCO1B1 gene polymorphisms with toxicity response of high dose methotrexate chemotherapy in childhood acute lymphoblastic leukemia. *Int J Clin Exp Med* 8(4):6109–6113
20. Yasuda SU, Zhang L, Huang SM (2008) The role of ethnicity in variability in response to drugs: focus on clinical pharmacology studies. *Clin Pharmacol Ther* 84(3):417–423. <https://doi.org/10.1038/clpt.2008.141>
21. Faganel Kotnik B, Grabnar I, Bohanec Grabar P, Dolzan V, Jazbec J (2011) Association of genetic polymorphism in the folate metabolic pathway with methotrexate pharmacokinetics and toxicity in childhood acute lymphoblastic leukaemia and malignant lymphoma. *Eur J Clin Pharmacol* 67(10):993–1006. <https://doi.org/10.1007/s00228-011-1046-z>
22. Kim IW, Yun HY, Choi B, Han N, Park SY, Lee ES, Oh JM (2012) ABCB1 C3435T genetic polymorphism on population pharmacokinetics of methotrexate after hematopoietic stem cell transplantation in Korean patients: a prospective analysis. *Clin Ther* 34(8):1816–1826. <https://doi.org/10.1016/j.clinthera.2012.06.022>
23. Lui G, Treluyer JM, Fresneau B, Piperno-Neumann S, Gaspar N, Corradini N, Gentet JC, Marec Berard P, Laurence V, Schneider P, Entz-Werle N, Pacquement H, Millot F, Taque S, Freycon C, Lervat C, Le Deley MC, Mahier Ait Oukhatar C, Brugières L, Le Teuff G, Bouazza N, Sarcoma Group of U (2018) A pharmacokinetic and pharmacogenetic analysis of osteosarcoma patients treated with high-dose methotrexate: data from the OS2006/sarcoma-09 trial. *J Clin Pharmacol* 58(12):1541–1549. <https://doi.org/10.1002/jcph.1252>
24. Cheah CY, Herbert KE, O'Rourke K, Kennedy GA, George A, Fedele PL, Gilbertson M, Tan SY, Ritchie DS, Opat SS, Prince HM, Dickinson M, Burbury K, Wolf M, Januszewicz EH, Tam CS, Westerman DA, Carney DA, Harrison SJ, Seymour JF (2014) A multicentre retrospective comparison of central nervous system prophylaxis strategies among patients with high-risk diffuse large B-cell lymphoma. *Br J Cancer* 111(6):1072–1079. <https://doi.org/10.1038/bjc.2014.405>
25. Hoang-Xuan K, Bessell E, Bromberg J, Hottinger AF, Preusser M, Ruda R, Schlegel U, Siegal T, Soussain C, Abacioglu U, Casoux N, Deckert M, Dirven CM, Ferreri AJ, Graus F, Henriksson R, Herrlinger U, Taphoorn M, Soffiatti R, Weller M, European Association for Neuro-Oncology Task Force on Primary CNSL (2015) Diagnosis and treatment of primary CNS lymphoma in immunocompetent patients: guidelines from the European Association for Neuro-Oncology. *Lancet Oncol* 16(7):e322–e332. [https://doi.org/10.1016/S1470-2045\(15\)00076-5](https://doi.org/10.1016/S1470-2045(15)00076-5)
26. Woessmann W, Seidemann K, Mann G, Zimmermann M, Burkhardt B, Oschlies I, Ludwig WD, Klingebiel T, Graf N, Gruhn B, Juergens H, Niggli F, Parwaresch R, Gadner H, Riehm H, Schrappe M, Reiter A, Group BFM (2005) The impact of the methotrexate administration schedule and dose in the treatment of children and adolescents with B-cell neoplasms: a report of the BFM Group Study NHL-BFM95. *Blood* 105(3):948–958. <https://doi.org/10.1182/blood-2004-03-0973>
27. Moricke A, Reiter A, Zimmermann M, Gadner H, Stanulla M, Dordelmann M, Loning L, Beier R, Ludwig WD, Ratei R, Harbott J, Boos J, Mann G, Niggli F, Feldges A, Henze G, Welte K, Beck JD, Klingebiel T, Niemeyer C, Zintl F, Bode U, Urban C, Wehinger H, Niethammer D, Riehm H, Schrappe M, German-Austrian-Swiss ALLBFMSG (2008) Risk-adjusted therapy of acute lymphoblastic leukemia can decrease treatment burden and improve survival: treatment results of 2169 unselected pediatric and adolescent patients enrolled in the trial ALL-BFM 95. *Blood* 111(9):4477–4489. <https://doi.org/10.1182/blood-2007-09-112920>
28. Jaccard A, Gachard N, Marin B, Rogez S, Audrain M, Suarez F, Tilly H, Morschhauser F, Thieblemont C, Ysebaert L, Devidas A, Petit B, de Leval L, Gaulard P, Feuillard J, Bordessoule D, Hermine O, Gela IG (2011) Efficacy of L-asparaginase with methotrexate and dexamethasone (AspaMetDex regimen) in patients with refractory or relapsing extranodal NK/T-cell lymphoma, a phase 2 study. *Blood* 117(6):1834–1839. <https://doi.org/10.1182/blood-2010-09-307454>
29. Dupuis C, Mercier C, Yang C, Monjanel-Mouterde S, Ciccolini J, Fanciullino R, Pourroy B, Deville JL, Duffaud F, Bagarry-Liegey D, Durand A, Iliadis A, Favre R (2008) High-dose methotrexate in adults with osteosarcoma: a population pharmacokinetics study and validation of a new limited sampling strategy. *Anticancer Drugs* 19(3):267–273
30. Keizer RJ, Karlsson MO, Hooker A (2013) Modeling and simulation workbench for NONMEM: tutorial on Pirana, P<sub>S</sub>N, and



- Xpose. *CPT Pharmacomet Syst Pharmacol* 2:e50. <https://doi.org/10.1038/psp.2013.24>
31. Karlsson MO, Savic RM (2007) Diagnosing model diagnostics. *Clin Pharmacol Ther* 82(1):17–20. <https://doi.org/10.1038/sj.clpt.6100241>
  32. Levey AS, Stevens LA, Schmid CH, Zhang YL, Castro AF 3rd, Feldman HI, Kusek JW, Eggers P, Van Lente F, Greene T, Coresh J, Ckd EPI (2009) A new equation to estimate glomerular filtration rate. *Ann Intern Med* 150(9):604–612. <https://doi.org/10.7326/0003-4819-150-9-200905050-00006>
  33. Yafune A, Ishiguro M (1999) Bootstrap approach for constructing confidence intervals for population pharmacokinetic parameters. I: a use of bootstrap standard error. *Stat Med* 18(5):581–599
  34. Bergstrand M, Hooker AC, Wallin JE, Karlsson MO (2011) Prediction-corrected visual predictive checks for diagnosing nonlinear mixed-effects models. *AAPS J* 13(2):143–151. <https://doi.org/10.1208/s12248-011-9255-z>
  35. Martinez D, Muhrez K, Woillard JB, Berthelot A, Gyan E, Choquet S, Andres CR, Marquet P, Barin-Le Guellec C (2018) Endogenous metabolites-mediated communication between OAT1/OAT3 and OATP1B1 may explain the association between SLCO1B1 SNPs and methotrexate toxicity. *Clin Pharmacol Ther* 104(4):687–698. <https://doi.org/10.1002/cpt.1008>
  36. Woillard JB, Debord J, Benz-de-Bretagne I, Saint-Marcoux F, Turlure P, Girault S, Abraham J, Choquet S, Marquet P, Barin-Le Guellec C (2017) A time-dependent model describes methotrexate elimination and supports dynamic modification of MRP2/ABCC2 activity. *Ther Drug Monit* 39(2):145–156. <https://doi.org/10.1097/FTD.0000000000000381>
  37. Faltaos DW, Hulot JS, Urien S, Morel V, Kaloshi G, Fernandez C, Xuan KH, Leblond V, Lechat P (2006) Population pharmacokinetic study of methotrexate in patients with lymphoid malignancy. *Cancer Chemother Pharmacol* 58(5):626–633. <https://doi.org/10.1007/s00280-006-0202-0>
  38. Mei S, Li X, Jiang X, Yu K, Lin S, Zhao Z (2018) Population pharmacokinetics of high-dose methotrexate in patients with primary central nervous system lymphoma. *J Pharm Sci* 107(5):1454–1460. <https://doi.org/10.1016/j.xphs.2018.01.004>
  39. Zhang W, Zhang Q, Tian X, Zhao H, Lu W, Zhen J, Niu X (2015) Population pharmacokinetics of high-dose methotrexate after intravenous administration in Chinese osteosarcoma patients from a single institution. *Chin Med J (Engl)* 128(1):111–118. <https://doi.org/10.4103/0366-6999.147829>
  40. Simon N, Marsot A, Villard E, Choquet S, Khe HX, Zahr N, Lechat P, Leblond V, Hulot JS (2013) Impact of ABCC2 polymorphisms on high-dose methotrexate pharmacokinetics in patients with lymphoid malignancy. *Pharmacogenomics J* 13(6):507–513. <https://doi.org/10.1038/tpj.2012.37>
  41. Aumente D, Buelga DS, Lukas JC, Gomez P, Torres A, Garcia MJ (2006) Population pharmacokinetics of high-dose methotrexate in children with acute lymphoblastic leukaemia. *Clin Pharmacokinet* 45(12):1227–1238. <https://doi.org/10.2165/00003088-200645120-00007>
  42. Colom H, Farre R, Soy D, Peraire C, Cendros JM, Pardo N, Torrent M, Domenech J, Mangués MA (2009) Population pharmacokinetics of high-dose methotrexate after intravenous administration in pediatric patients with osteosarcoma. *Ther Drug Monit* 31(1):76–85. <https://doi.org/10.1097/FTD.0b013e3181945624>
  43. Min Y, Qiang F, Peng L, Zhu Z (2009) High dose methotrexate population pharmacokinetics and Bayesian estimation in patients with lymphoid malignancy. *Biopharm Drug Dispos* 30(8):437–447. <https://doi.org/10.1002/bdd.678>
  44. Odoul F, Le Guellec C, Lamagnere JP, Breilh D, Saux MC, Painaud G, Autret-Leca E (1999) Prediction of methotrexate elimination after high dose infusion in children with acute lymphoblastic leukaemia using a population pharmacokinetic approach. *Fundam Clin Pharmacol* 13(5):595–604
  45. Plard C, Bressolle F, Fakhoury M, Zhang D, Yacouben K, Rieutord A, Jacqz-Aigrain E (2007) A limited sampling strategy to estimate individual pharmacokinetic parameters of methotrexate in children with acute lymphoblastic leukemia. *Cancer Chemother Pharmacol* 60(4):609–620. <https://doi.org/10.1007/s00280-006-0394-3>

**Publisher's Note** Springer Nature remains neutral with regard to jurisdictional claims in published maps and institutional affiliations.